

# CHEM**BIO**CHEM

## Supporting Information

### **Construction of a Holliday Junction in Small Circular DNA Molecules for Stable Motifs and Two-Dimensional Lattices**

Xin Guo,<sup>[a]</sup> Xue-Mei Wang,<sup>[a]</sup> Shuai Wei,<sup>[b]</sup> and Shou-Jun Xiao<sup>\*[a, c]</sup>

cbic\_201800122\_sm\_miscellaneous\_information.pdf

## SUPPORTING INFORMATION

## Table of Contents

1 Experimental Procedures.....	2
2 Persistence Length Calculation.....	3
3 Preparation of Circular DNA .....	4
4 Native PAGE of Fully Associated c64nt Duplexes with Respective Central Symmetric Nick Pairs.....	5
5 Schematic Model of Chiral cDAO-c84nt Tile .....	5
6 Diagrams of DNA Structure Designs.....	6
7 Agarose Gel Electrophoresis of Finite cDAO-c64nt-O and cDAO-c74&c84nt-O .....	10
8 Additional AFM Images. ....	11

## 1 Experimental Procedures

**Sample preparation.** All DNA strands were provided with denaturing PAGE purification by Sangon Biotech (www.sangon.com) without further purification. Detailed DNA sequences and structural designs are shown in the following Sections. To assemble the structures, DNA strands were mixed in an equimolar stoichiometric ratio from a 10  $\mu\text{M}$  stock in 1  $\times$  TAE buffer (40 mM Tris, 40 mM HAc, 1 mM EDTA, pH=8.0) supplemented with 12.5 mM  $\text{Mg}(\text{Ac})_2$  (abbreviated as TAE•Mg buffer). For c64nt nanowire, c84nt nanowire and acDAO-c64nt-E, the final concentration of each strand was adjusted to 0.5  $\mu\text{M}$ . For infinite cDAO-c64nt-E, cDAO-c64nt-O, cDAO-c84nt-E, and cDAO-c84nt-O assemblies, the final products were mixed with two separated sub-tiles, the concentration of each strand in the precursor sub-tile solution was 0.5  $\mu\text{M}$  and in the final product solution was 0.25  $\mu\text{M}$ . For finite cDAO-c64nt-O and cDAO-c74&c84nt-O assemblies, the final products were mixed with  $x$  sub-tiles ( $x$  depends on the size design) having the same concentration and volume, the concentration of each strand in the final product solution was 50 nM, whereas in the precursor sub-tile solution was 50x nM.

**Annealing ramps.** c64nt nanowire, c84nt nanowire and acDAO-c64nt-E were annealed in a thermo bottle from 95  $^{\circ}\text{C}$  to 25  $^{\circ}\text{C}$  in 48 hours respectively. The sub-tiles of cDAO-c64nt and cDAO-c84nt were firstly annealed in a PCR thermo cycler using a fast linear cooling step from 95  $^{\circ}\text{C}$  to 25  $^{\circ}\text{C}$  in about 2.5 hours. Then the mixture of each assembly was annealed in a PCR thermo cycler using a cooling step of staying at 50  $^{\circ}\text{C}$  for 2 hours and cooling down at a rate of 0.1  $^{\circ}\text{C}$  per 5 minutes to 20  $^{\circ}\text{C}$ , about 24 hours in total.

**Native PAGE analysis.** To analyze the stable circular tiles, 5  $\mu\text{L}$  of the annealed DNA structure was added with 1  $\mu\text{L}$  loading dye (0.05% bromophenol blue, 0.05% xylene cyanol FF, 60% glycerol, 10 mM Tris-HCl, 60 mM EDTA, pH=7.6) and then subjected to 10% native PAGE in TAE•Mg buffer at 60 volts for about 4 hours in an ice water bath. Then the gel was dyed with GelRed™ about 30 minutes and analyzed under UV light.

**Purification of Finite Lattices.** The finite lattices of 5  $\times$  6 patches of cDAO-c64nt-O and 5  $\times$  6 patches of cDAO-c74&c84nt-O were purified with both agarose gel electrophoresis and PEG precipitation.<sup>[1]</sup> 1) Agarose gel electrophoresis: Samples were subjected to 2% native agarose gel electrophoresis at 50 volts for 2 hours (gel prepared in 0.5  $\times$  TBE buffer supplemented with 12.5 mM  $\text{Mg}(\text{Ac})_2$  and 2  $\mu\text{L}$  GelRed) in an ice water bath. Then, the target gel bands were excised and placed into a Freeze 'N Squeeze column (Bio-Rad Laboratories, Inc.). The gel bands were cut to fine pieces in the column and the column was then centrifuged at 7000 g for 5 minutes. Sample solutions that were extracted through the column were collected for AFM imaging. 2) PEG precipitation: The reaction mixtures were mixed 1:1 (v/v) with 15% PEG8000 (w/v) buffer (20 mM  $\text{Mg}(\text{Ac})_2$ , 5 mM Tris, 1 mM EDTA and 505 mM NaCl). Then the solution was spun at 18000 g and 4  $^{\circ}\text{C}$  for 30 minutes. The supernatant was removed using a pipette. The pellet was dissolved in TAE•Mg buffer for AFM imaging.

**AFM imaging.** All AFM images of infinite DNA lattices were obtained in "ScanAsyst mode in air" (Dimension FastScan, Bruker) with FastScan-C tips (Bruker). The sample preparation procedure is: a 2  $\mu\text{L}$  annealed sample was deposited onto a freshly cleaved mica surface (Ted Pella), stayed 2 minutes for adsorption of DNA lattices to the mica surface, then the sample was washed off by 50  $\mu\text{L}$  deionized water twice and dried by compressed air. AFM images of finite DNA lattices were obtained in "ScanAsyst mode in fluid" with ScanAsyst-Fluid+ tips. The sample preparation procedure is: a 2  $\mu\text{L}$  sample was deposited onto a freshly cleaved mica surface (Ted Pella), stayed 0.5 min for adsorption, then 80  $\mu\text{L}$  TAE•Mg buffer was added on top of the sample and an extra 40  $\mu\text{L}$  of the same buffer was added on the AFM tip.

## SUPPORTING INFORMATION

## 2 Persistence Length Calculation

As we have shown in the native PAGE results of Figure 2B, the asymmetric tile of acDAO-c64nt is stable and rigid as well as cDAO-c64nt. With the predictable curvature of acDAO-c64nt and linear connections, we assembled curved acDAO-c64nt-E nanowires including nanorings, nanoarcs, and nanospirals in Figure 3D and Figure S23. Statistically, the one-tile wide curved nanowires are composed of 10 to 20 tiles. As the rigidity of tiles is considered as one of the most important parameters in assembling perfect single crystalline DNA lattices, we tried to quantitatively evaluate it as described below.

From the well-known worm-like-chain model, the rigidity of a polymer can be well characterized quantitatively by the persistence length in its longitudinal direction. A variety of methods have been established to estimate the persistence length of a polymer. Among them, the microscopic images based method has been well accepted.<sup>[2-6]</sup> Generally if a polymer is captured in microscopes with random curvatures along the worm-like chains, the persistence length of the polymer can be calculated directly by some open-source softwares such as the FiberApp.<sup>[6]</sup> The persistence length of a polymer is formally defined via the Bond Correlation Function in 3D as the length over which angular correlations in the tangent direction decrease by  $e$  times, as described in Equation 1.<sup>[2]</sup>

$$\langle \cos\theta \rangle = e^{-\frac{l}{2\lambda}} \quad (1)$$

where  $\langle \dots \rangle$  denotes the ensemble average,  $\theta$  is the angle between unit tangent vectors along a fibril contour separated by an arc length  $l$  and  $\lambda$  is the persistence length.

We designed an intrinsic curvature for acDAO-c64nt, which is the major difference from natural DNA fibers with random curvatures along their worm-like chains. When a polymer itself has an intrinsic curvature, the persistence length estimated from the microscopic images is called apparent persistence length ( $\lambda_a$ ). Since the intrinsic curvature contributes largely as an intrinsic persistence length ( $\lambda_i$ ) to the experimentally determined apparent persistence length ( $\lambda_a$ ), a so-called dynamic persistence length ( $\lambda_d$ ) has been well accepted to represent the rigidity of the polymer in Equation 2.<sup>[3,4]</sup>

$$\frac{1}{\lambda_a} = \frac{1}{\lambda_i} + \frac{1}{\lambda_d} \quad (2)$$

Thus, to determine  $\lambda_d$ , we have to calculate both  $\lambda_i$  and  $\lambda_a$ .

The intrinsic persistence length of  $\lambda_i$  was calculated to be 31.20 nm from Equation 1, where the independent variables can be simply calculated as shown in Figure S3: the central arc length ( $l$ ) is 10.88 nm, the radius ( $r$ ) is 18.96 nm,  $\langle \cos\theta \rangle = \cos\theta = \cos(l/r) = 0.84$ . Appreciating the open-source software of FiberApp,<sup>[6]</sup> we employed the most widely used approach of the mean-squared end-to-end distance (MSED) between contour segments to calculate  $\lambda_a$  for 108 randomly picked fiber-like structures (Figure S1). The result of  $\lambda_a$  was shown in Figure S2, which was converged at 29.86 nm. Therefore, according to Equation 2,  $\lambda_d$  was calculated to be 695.2 nm. The estimated persistence length of around 700 nm of acDAO-c64nt-E nanowires, 14 times of 50 nm of a linear DNA double helix's persistence length, is reasonable because it is in accordance with the rigid and straight rod model suggested from native PAGE results in Figure 2B, and also comparable to the previously reported persistence length in the range of 2.0 to 30.0  $\mu\text{m}$  for nanotubes built from DAE-E and DNA origami.<sup>[7,8]</sup>

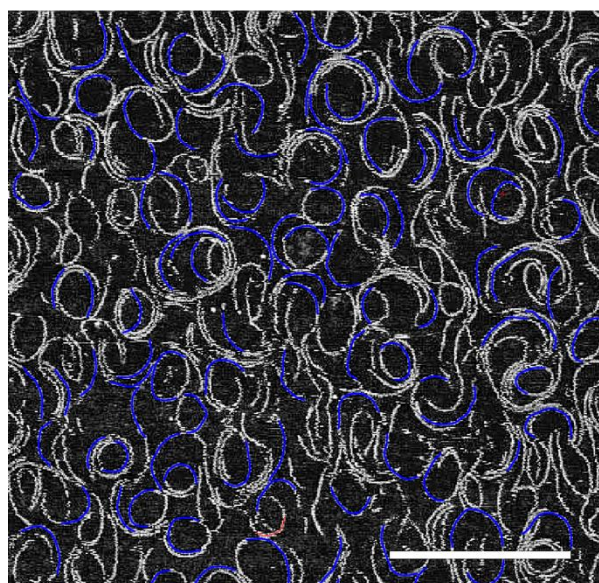


**Figure S1.** Random selections of curved nanowires by FiberApp.<sup>[6]</sup> 108 pieces of curved nanowires marked with blue in the AFM image of acDAO-c64nt-E nanowires were randomly selected for estimation of their persistence length. The scale bar is 300 nm.

## SUPPORTING INFORMATION

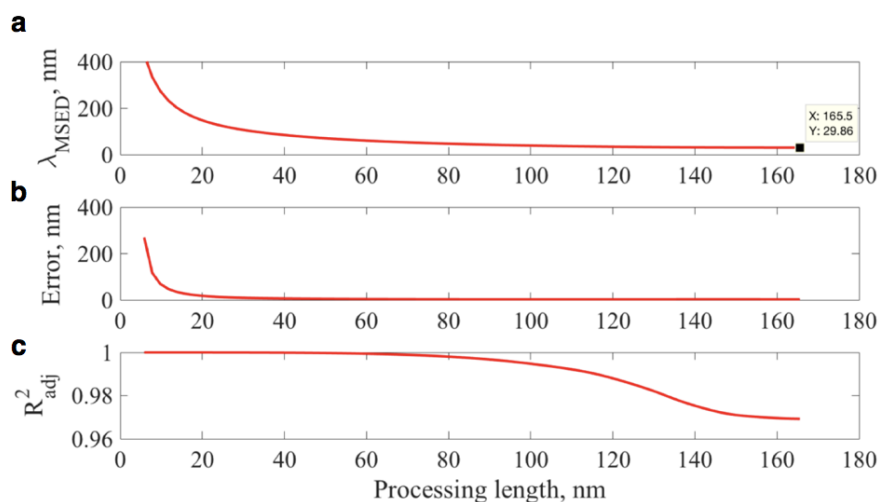


**Figure S2.** FiberApp simulation of the apparent persistence length ( $\lambda_a$ ) by MSED. (a)  $\lambda_a$  (apparent persistence length in nm) calculated by MSED versus the processing length. (b) The error (in nm) of  $\lambda_a$  estimation by MSED versus the processing length. (c) Coefficient of determination (1.0 means perfect fitting) for the  $\lambda_a$  estimation versus the processing length. The estimation results are based on the 108 randomly selected fibrils from the AFM image of Figure S1 by the FiberApp software.

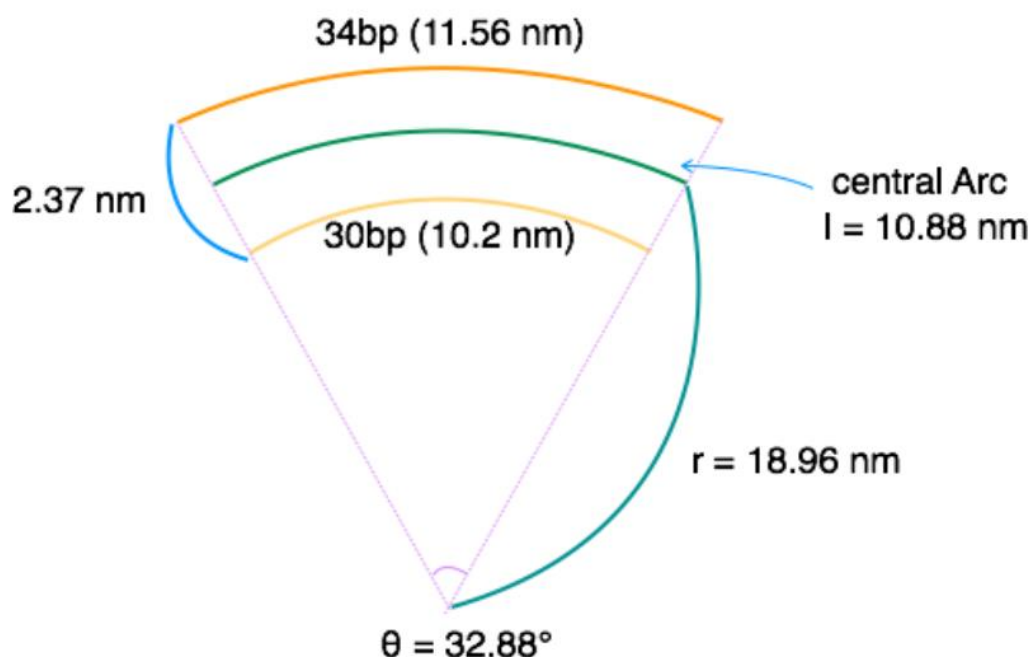


**Figure S3.** Schematic geometries of acDAO-c64nt for calculation of the intrinsic persistence length ( $\lambda_i$ ). We take 2.37 nm as the diameter of double-stranded B-form DNA because the curved nanowires of acDAO-c64nt-E in Figure S1 were imaged by AFM in air.

### 3 Preparation of Circular DNA

The circular DNAs of c64nt, c74nt and c84nt were circularized by T4 DNA ligase. Firstly, a 5'-phosphorylated DNA strand (3.5  $\mu\text{M}$ ) and its corresponding 20 nt splint DNA strand (4.5  $\mu\text{M}$ ) were mixed in 80  $\mu\text{L}$  TE buffer (pH = 8.0). The mixture was heated to 95  $^\circ\text{C}$  for 5 minutes, then cooled down to room temperature within 2 hours. After annealing, 10 $\times$ T4 buffer (660 mM Tris-HCl, 66 mM  $\text{MgCl}_2$ ,

## SUPPORTING INFORMATION

100 mM DTT, 1 mM ATP, 10  $\mu$ L) and T4 ligase (300 U/ $\mu$ L, 10  $\mu$ L) were added, and the mixture was incubated for 16 hours at 16  $^{\circ}$ C, followed by T4 ligase inactivation at 95  $^{\circ}$ C for 5 minutes. After ligation and inactivation, 10  $\mu$ L 10 $\times$  Exonuclease I buffer and 10  $\mu$ L Exonuclease I (5 U/ $\mu$ L) were added to digest the remaining linear DNA templates and its corresponding splint strands by incubation at 37  $^{\circ}$ C for 30 minutes. The enzyme selectively digested the single-stranded DNA, and left the circularized DNA intact.

The circularized DNA strands were purified by denaturing polyacrylamide gel electrophoresis. The protocol is as follows: (1) purify the circularized DNA strands by 10% denaturing PAGE, using a constant voltage of 5V/cm for 2 hours; (2) cut out of the corresponding gel bands by a razor blade under UV light; (3) chop and crush the gel bands into fine pieces and transfer into a 2.0 mL Eppendorf tube; (4) add deionized water at least twice of the gel volume into the tube and shake at room temperature overnight; (5) filter to collect the supernatants, recovery any residual DNA by rinsing with small volume of deionized water and filter again to combine the supernatants; (6) extract the eluent with n-butanol to about 200  $\mu$ L; (7) add 500  $\mu$ L 100 % ethanol, 20  $\mu$ L 3M NaOAc (pH = 5.2) and store the tube at -20  $^{\circ}$ C for 2 hours; (8) centrifuge at 12000 g for 10 minutes at 4  $^{\circ}$ C and discard the supernatant; (9) add 600  $\mu$ L 75% ethanol (-20  $^{\circ}$ C) and centrifuge again to collect the pellet; (10) dry and store circular DNAs at -20  $^{\circ}$ C.

#### 4 Native PAGE of Fully Associated c64nt Duplexes with Respective Central Symmetric Nick Pairs

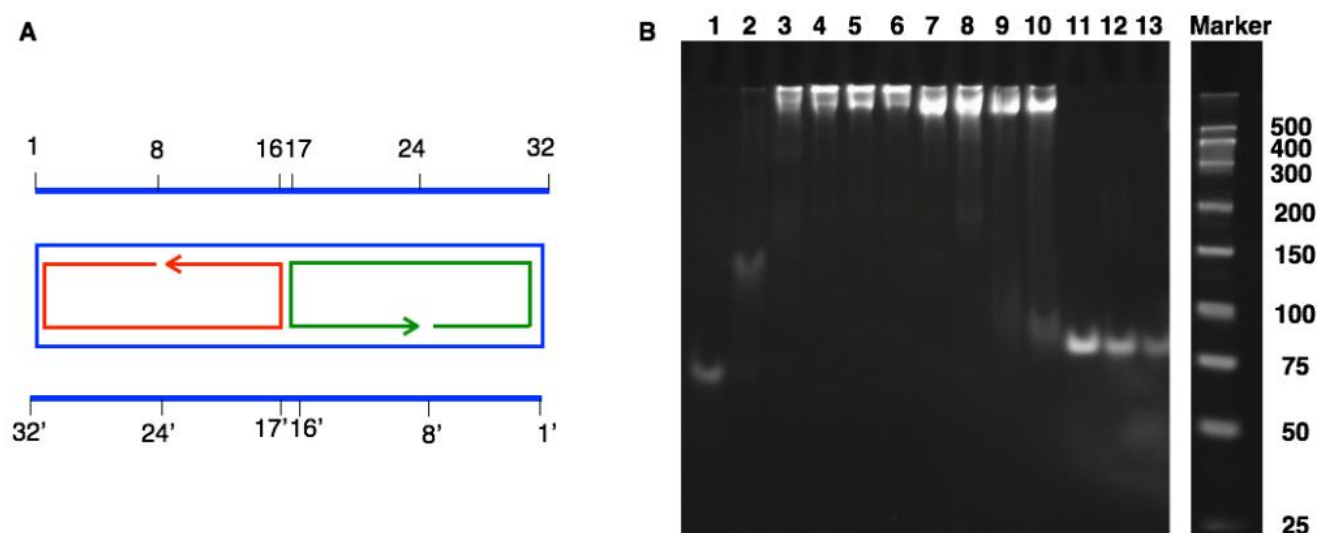


**Figure S4.** Native PAGE analysis of fully associated c64nt duplexes with respective central symmetric nick pairs. (A) The blue circle represents c64nt, the red and green strands represent two linear staple strands; these three strands construct fully associated c64nt duplexes with respective central symmetric nick pairs at different positions. The two thick blue segments with key ordinals above and below the fully associated c64nt duplex indicate sequential base pairs in the upper and lower duplexes respectively. A Holliday junction is formed at the center with coordinates of (16, 17, 16', 17'). The schematic drawing is actually "c64nt nanowire" in Figure 1 of the main text with a pair of two nicks placed at (8, 9) and (8', 9'). The folding structural diagram of c64nt nanowire is also shown in Figure S6. (B) The native PAGE results placing a pair of two central symmetric nicks at different positions. With a nick pair at  $\{(1, 32'), (1', 32)\}$ , it forms the tile of HJ-c64nt as in Figure 1 of the main text. When nick pairs are placed from  $\{(2, 3), (2', 3')\}$  to  $\{(14, 15), (14', 15')\}$ , their corresponding annealing products are shown in (B) from lane 1 to 13. Descriptions of the native PAGE results please refer to the main text.

#### 5 Schematic Model of Chiral cDAO-c84nt Tile

## SUPPORTING INFORMATION

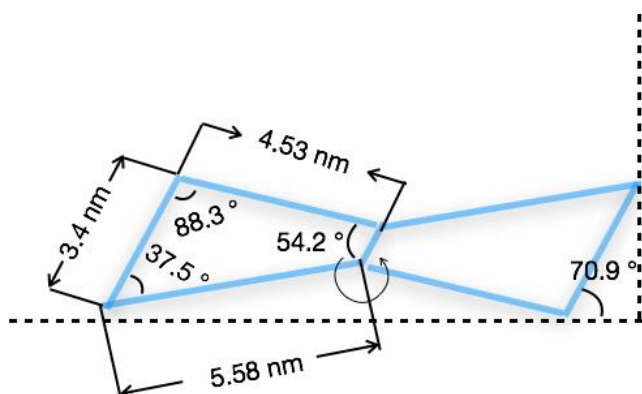


**Figure S5.** Chiral structure of cDAO-c84nt. The chiral tile model is suggested from the measured lattice parameters of cDAO-c84nt-E and also from the c84nt rotation direction labeled with a curved arrow. cDAO-c84nt is schematically represented with a pair of congruent hollow triangles forming a crossed quadrilateral, whose left and right bases are tilted  $70.9^\circ$  towards the horizontal direction in Figure 4 of the main text. Here HJ is emphasized with a short bar in the center, parallel to both left and right bases. The geometrical parameters of cDAO-c84nt were estimated as follows: the left base was a full pitch from design by  $10 \text{ bp} \times 0.34 \text{ nm/bp} = 3.4 \text{ nm}$ , the upper edge was estimated by  $(16.2 \text{ nm} - 21 \text{ bp} \times 0.34 \text{ nm/bp})/2 = 4.53 \text{ nm}$ , the lower edge was estimated by  $(18.3 \text{ nm} - 21 \text{ bp} \times 0.34 \text{ nm/bp})/2 = 5.58 \text{ nm}$ . The angles were calculated by trigonometric functions. Since the double DNA helices are considered as a worm-like chain with a Young's modulus on the order of 0.3-1 GPa, DNA strands will be stretched in some regions like at the junctions whereas compressed in other regions, therefore the edge lengths will be not identical even if they have the same number of base pairs. Each part of cDAO-c84nt can be stretched or compressed as a resonant structure to its balanced position in aqueous media. The chiral structure always remains because the stretching and compression are correlated in the resonant structure.

## 6 Diagrams of DNA Structure Designs

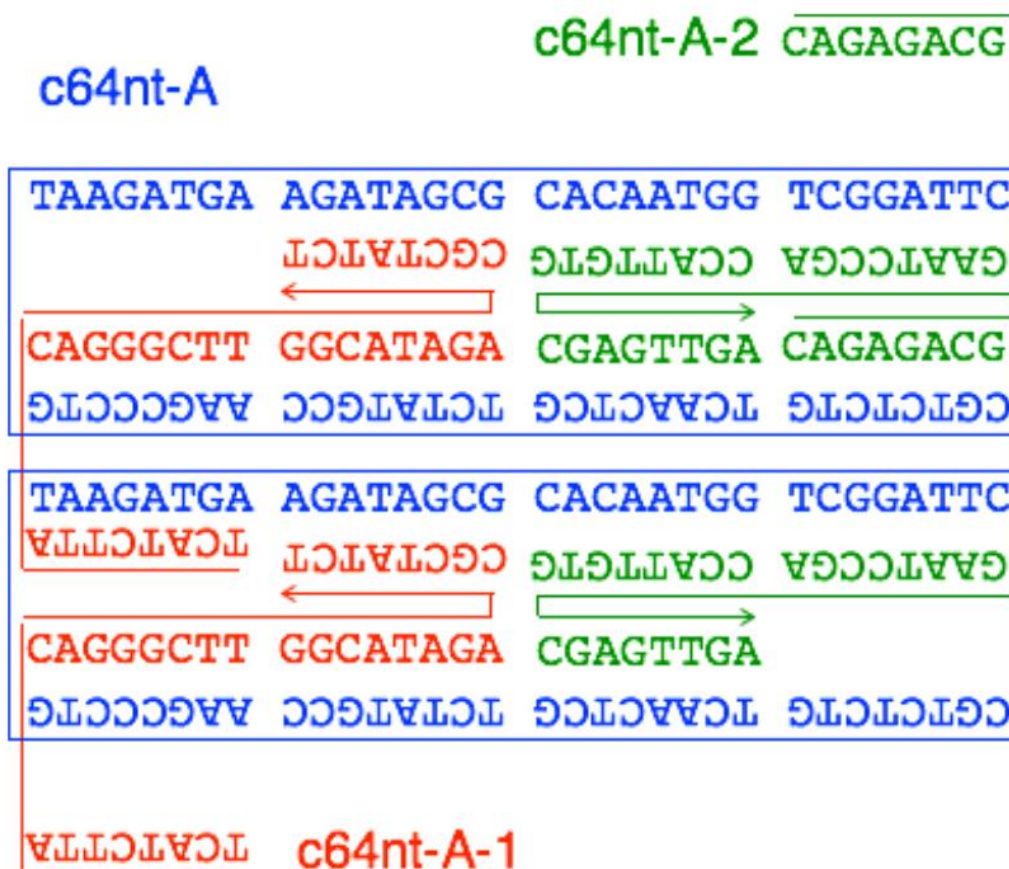


**Figure S6.** Detailed sequence design of c64nt nanowire.

SUPPORTING INFORMATION

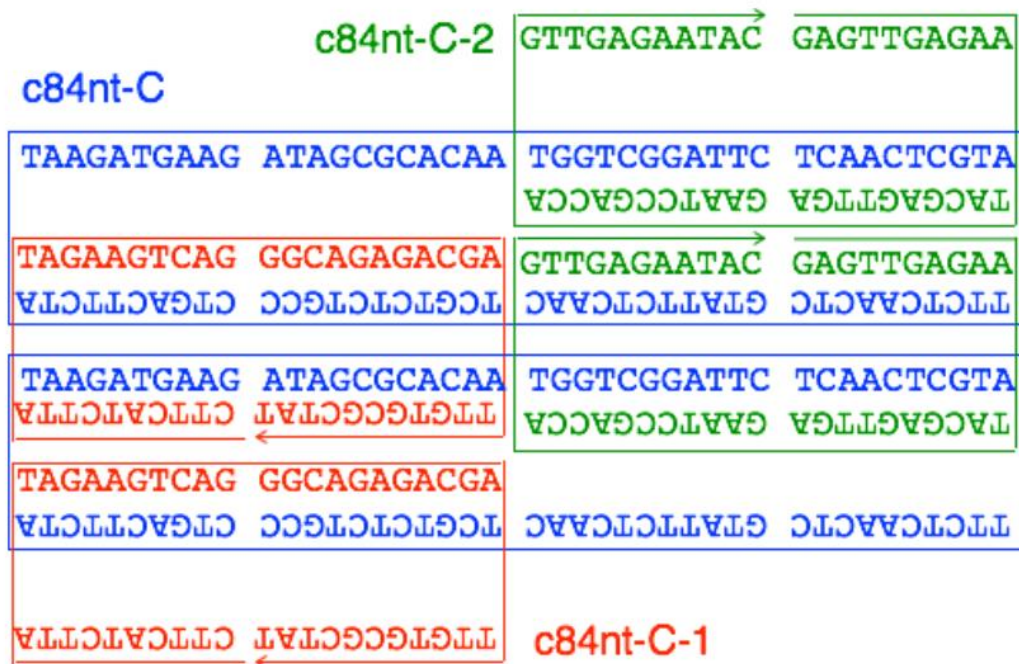


Figure S7. Detailed sequence design of c84nt nanowire.

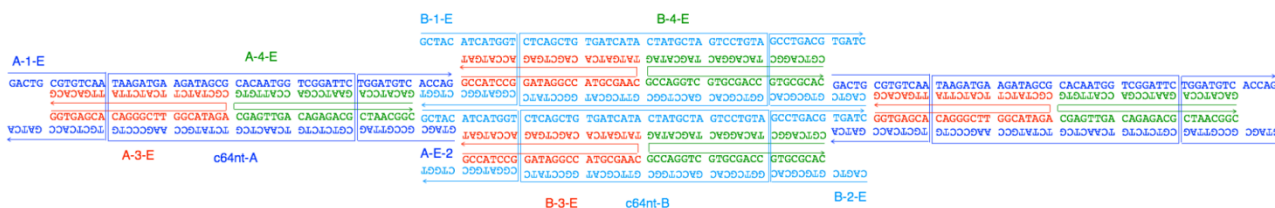


Figure S8. Detailed sequence design of cDAO-c64nt-E.

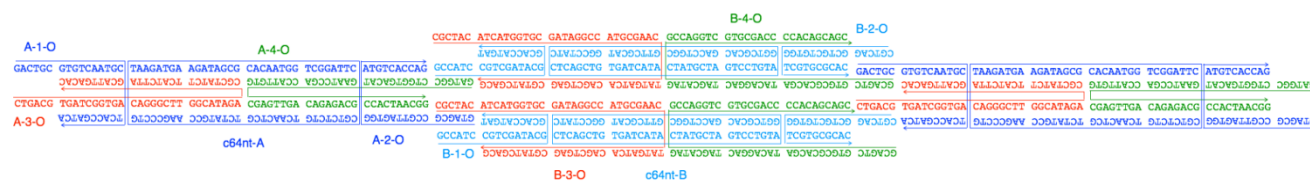
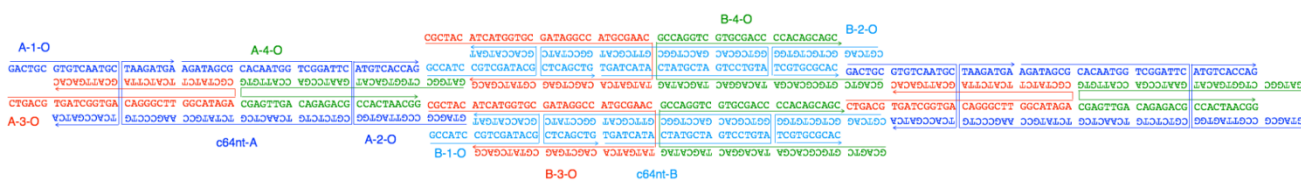
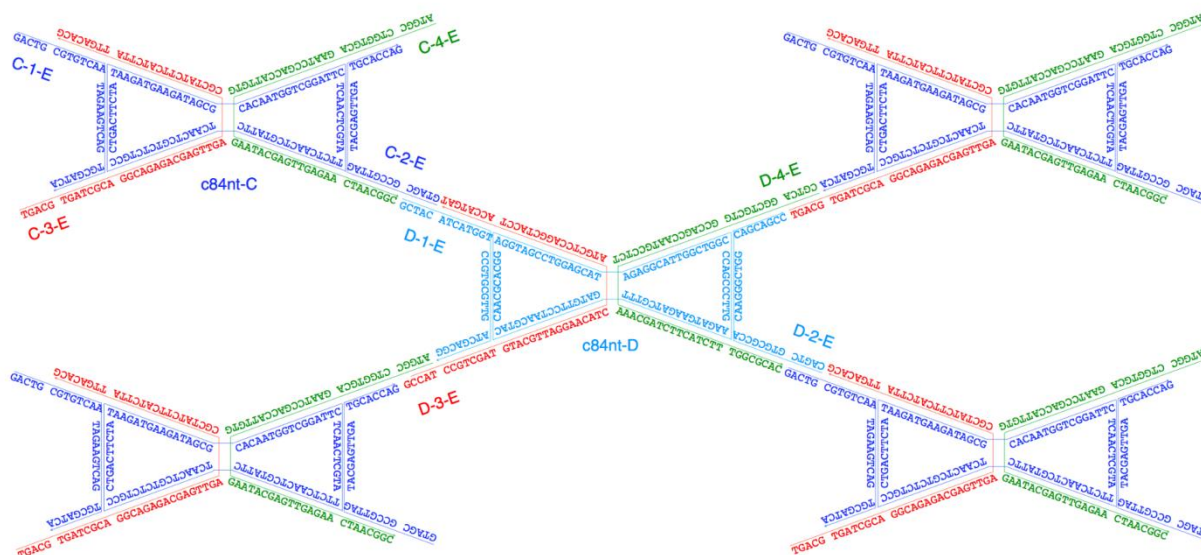


Figure S9. Detailed sequence design of cDAO-c64nt-O.



## SUPPORTING INFORMATION

**Figure S10.** Detailed sequence design of cDAO-64nt-O with a whole set of linear strands. This is a control experiment for the cDAO-c64nt-O 2D lattice. The design and sequences are the same as cDAO-c64nt-O except the circular c64nt scaffold is broken with a nick to a looped linear 64nt scaffold. Its assembly product is 2D amorphous aggregates along the double helical axes by AFM imaging in Figure S26.



**Figure S11.** Detailed sequence design of cDAO-c84nt-E.

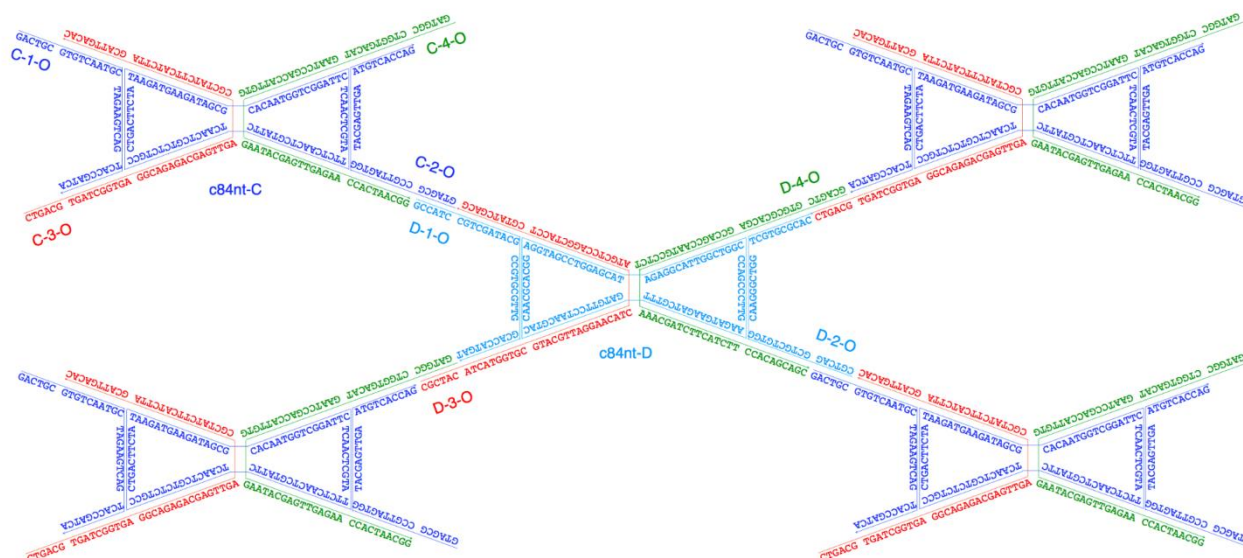


**Figure S12.** Detailed sequence design of cDAO-c84nt-O.



## SUPPORTING INFORMATION

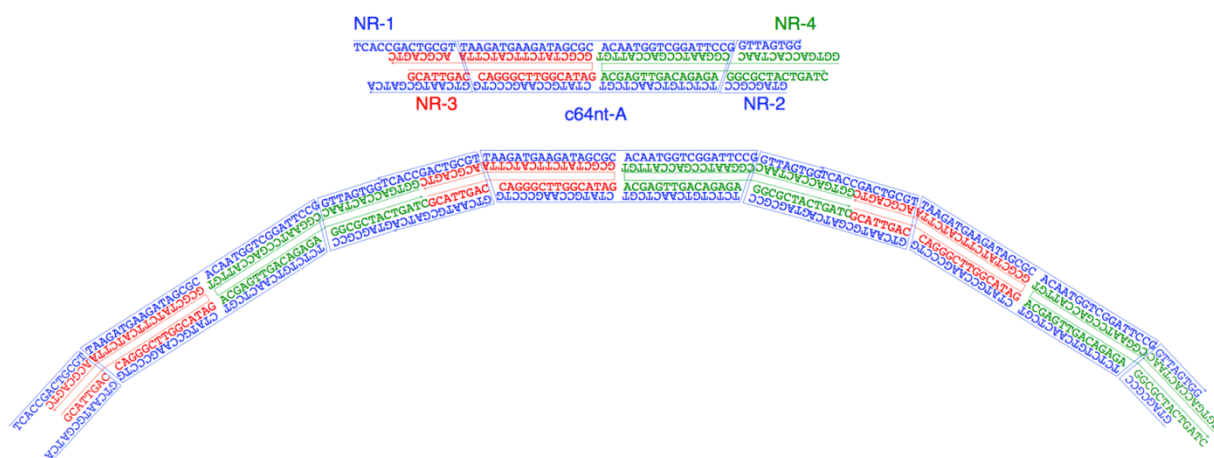


Figure S13. Detailed sequence design of acDAO-c64nt-E.

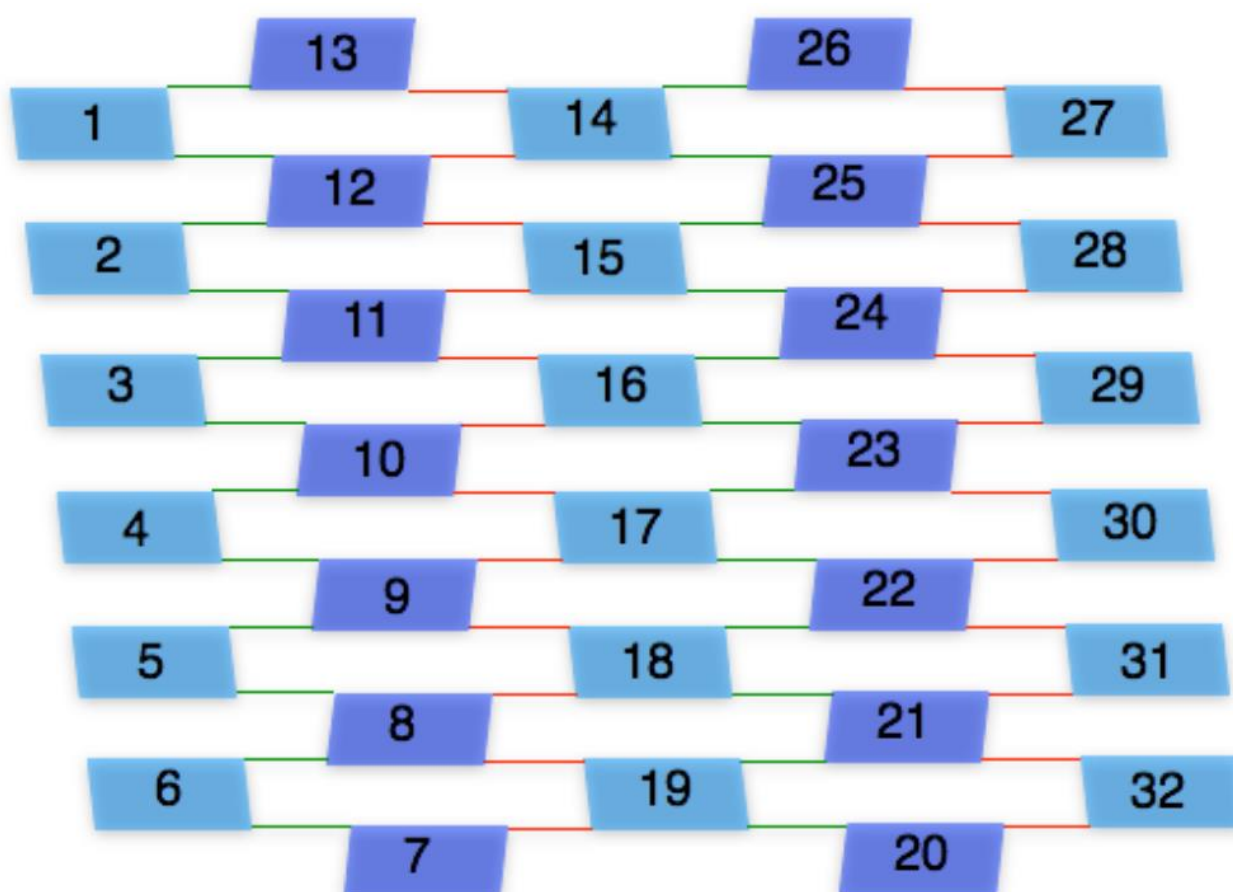
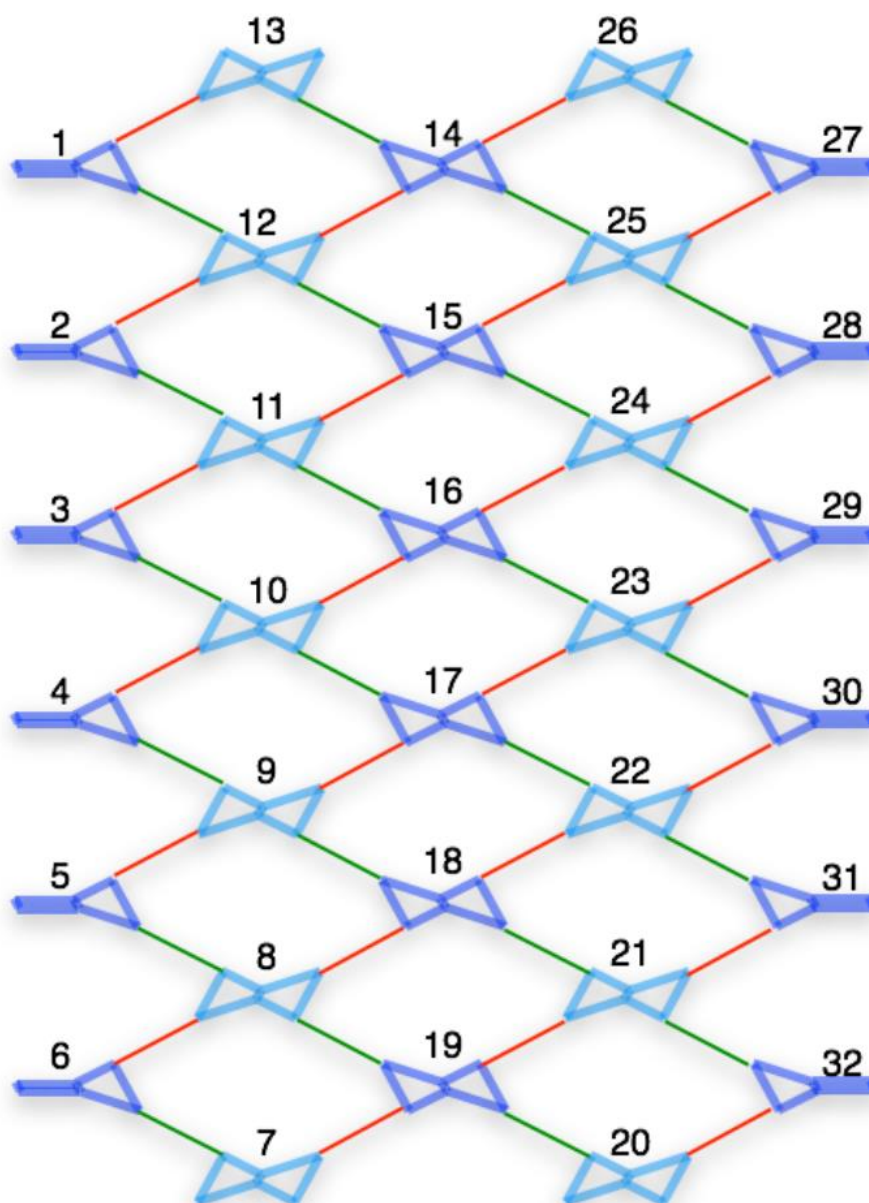


Figure S14. The scheme of finite 5x6 patches of cDAO-c64nt-O. The numbered blue blocks represent 32 different HJ-c64nt tiles. Two different colors of sky blue and deep blue distinguish the two different faces (or chiralities) of cDAO-c64nt. At both left and right edges of the structure the protruding strands were terminated with six thymines to prevent the inter-lattice  $\pi$ - $\pi$  edge-stacking. Only one sequence of c64nt was used, whereas the sticky ended overhangs were with different sequences, the individual tiles were annealed first respectively and then mixed together at 50 °C to grow the finite lattice. Each tile inside the diagram contains a c64nt and four linear staple strands, for example, tile 10 contains c64nt-A, H-L-10, H-R-10, M-L-10 and M-R-10 (10 means the tile number, H the helper staple strand, M the main staple strand, L the left side of the tile, R the right side of the tile). Each tile at both left and right edges contains a c64nt and three linear staple strands, for example, tile 1 contains c64nt-A, H-R-01, M-L-01 and M-R-01, tile 32 contains c64nt-A, H-L-32, M-L-32 and M-R-32. To enhance the cohesion strength, the sticky ends in the finite cDAO-c64nt-O are 10 nt long.

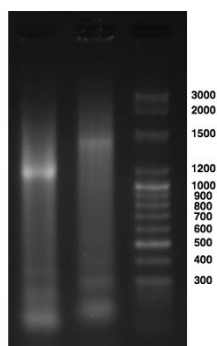
## SUPPORTING INFORMATION



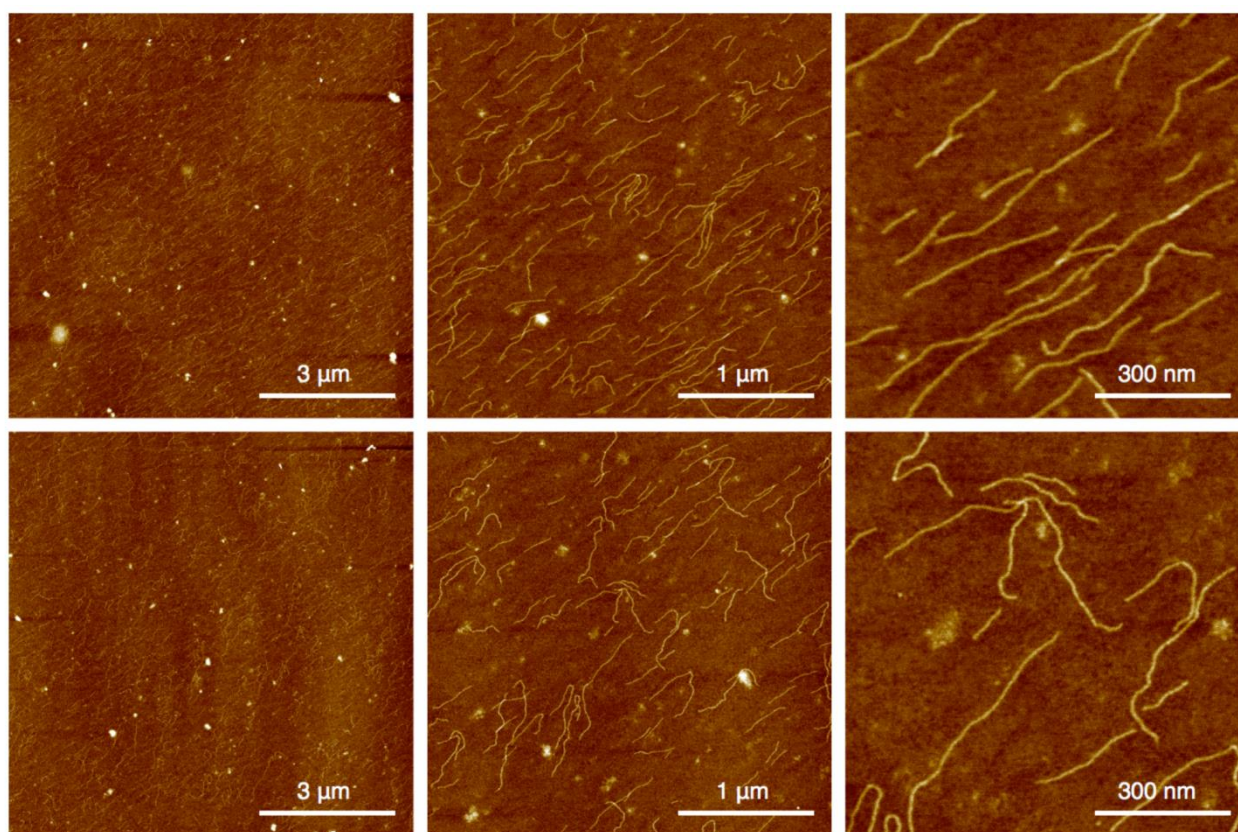
**Figure S15.** The scheme of finite 5x6 cDAO-c74&c84nt-O. The finite structure of cDAO-c74&c84nt-O is composed of 12 asymmetric cDAO-c74nt tiles, distributed on both left and right sides, and 20 cDAO-c84nt tiles inside the structure. Only one circular sequence of c74nt and one circular sequence of c84nt were used, whereas the sticky ended overhangs were with different sequences, the individual tiles were annealed first respectively and then mixed together at 50 °C to grow the finite lattice. The ending strands protruding from cDAO-c74nt tiles were terminated with six thymines to prevent the  $\pi$ - $\pi$  stacking of inter-lattice edges. Two different colors distinguish the two different faces of cDAO-c84nt. Each cDAO-c84nt contains a c84nt-C and four linear staple strands: H-L-N, H-R-N, M-L-N and M-R-N (N means the cDAO-c84nt tile number, H the helper staple strand, M the main staple strand, L the left side of the tile, R the right side of the tile). Each cDAO-c74nt contains a c74nt and three linear staple strands: H-L-N (or H-R-N), M-L-N and M-R-N (N means the cDAO-c74nt tile number, H the helper staple strand, M the main staple strand, L the left side of the tile, R the right side of the tile).

## 7 Agarose Gel Electrophoresis of Finite cDAO-c64nt-O and cDAO-c74&c84nt-O

## SUPPORTING INFORMATION



**Figure S16.** The agarose gel analysis of finite lattices of 5x6 cDAO-c64nt-O (left) and 5x6 cDAO-c74&c84nt-O (middle). We estimated the yields of 5x6 patches of cDAO-c64nt-O (left lane) and 5x6 patches of cDAO-c74&c84nt-O (middle lane) at around 30.0% and 23.5% from its band percentage in all bands of its lane by strength respectively with Image-J by supposing the grayscale strength represents the DNA quantity linearly.

**8 Additional AFM Images**

**Figure. S17.** AFM images of c64nt nanowire.

## SUPPORTING INFORMATION

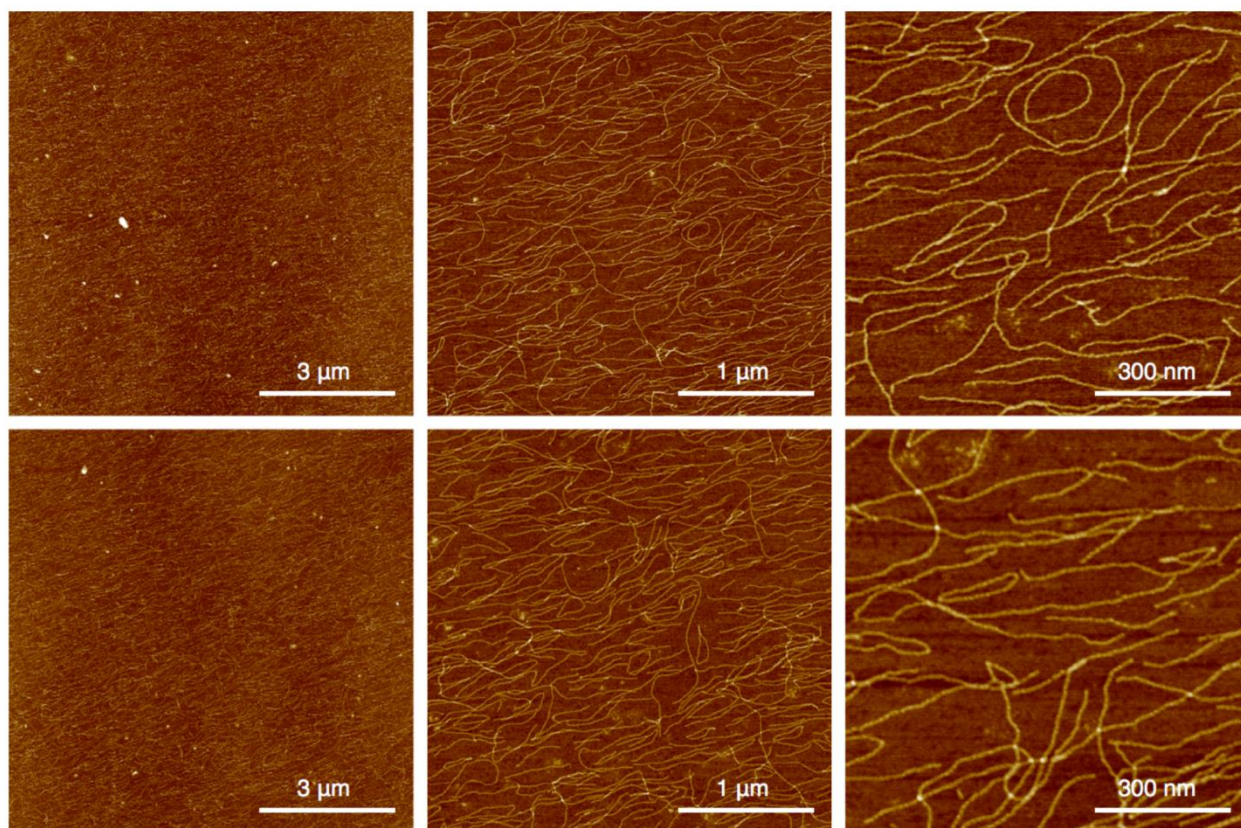


Figure. S18. AFM images of c84nt nanowire.

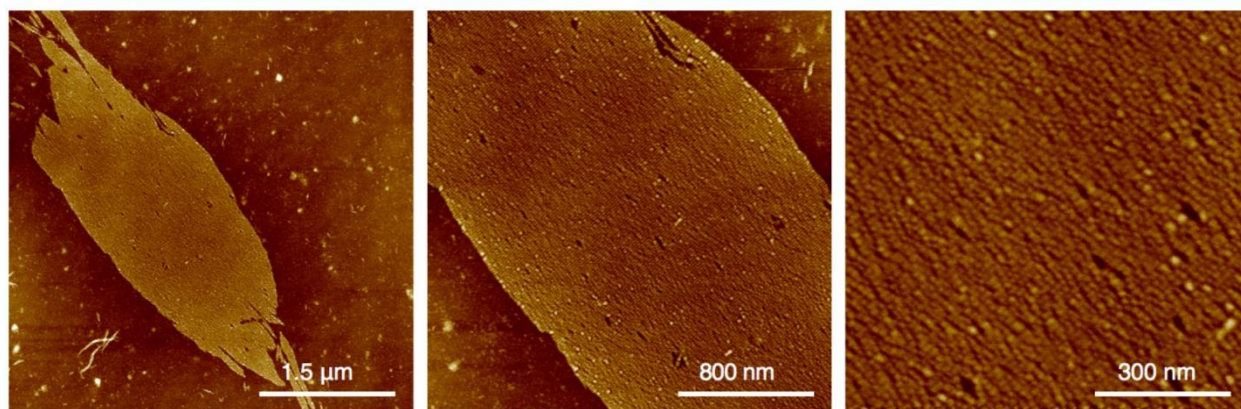


Figure. S19. AFM images of infinite cDAO-c64nt-E.

## SUPPORTING INFORMATION

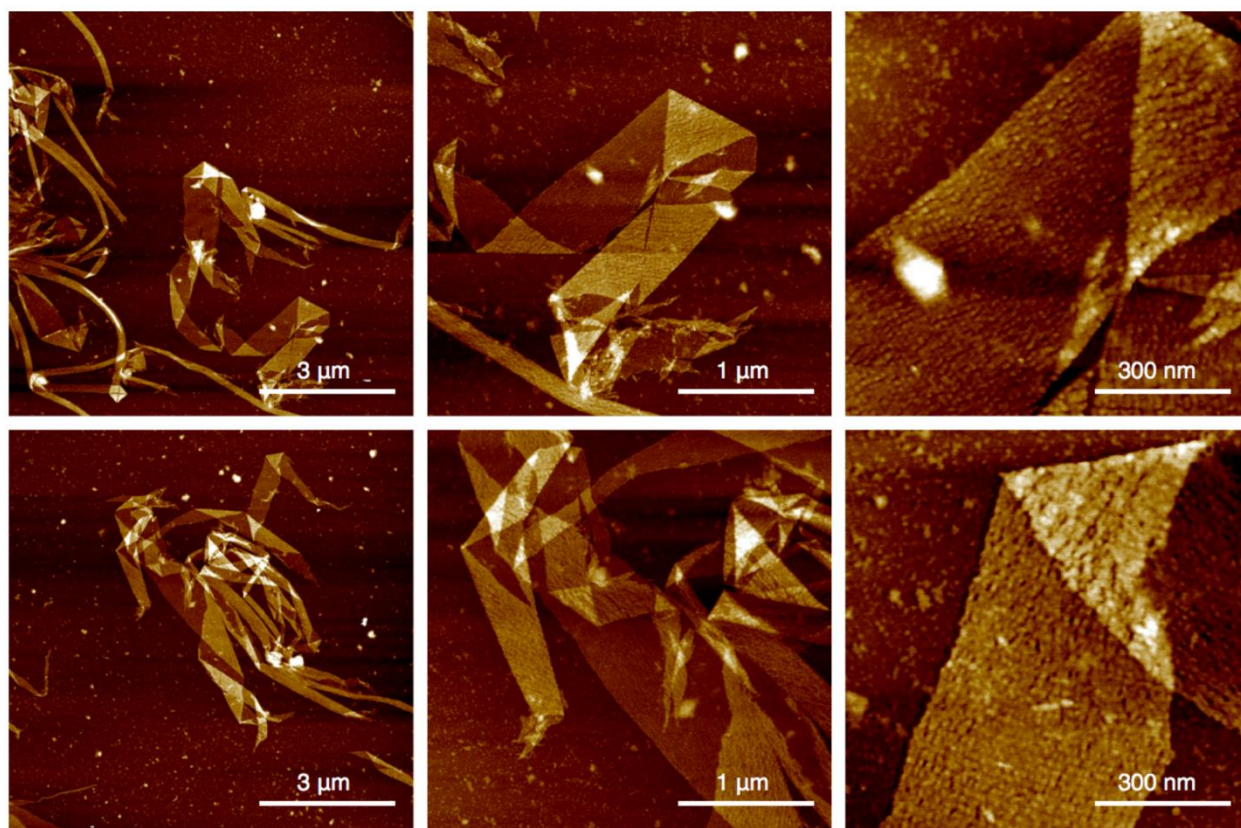


Figure. S20. AFM images of infinite cDAO-c64nt-O.

## SUPPORTING INFORMATION

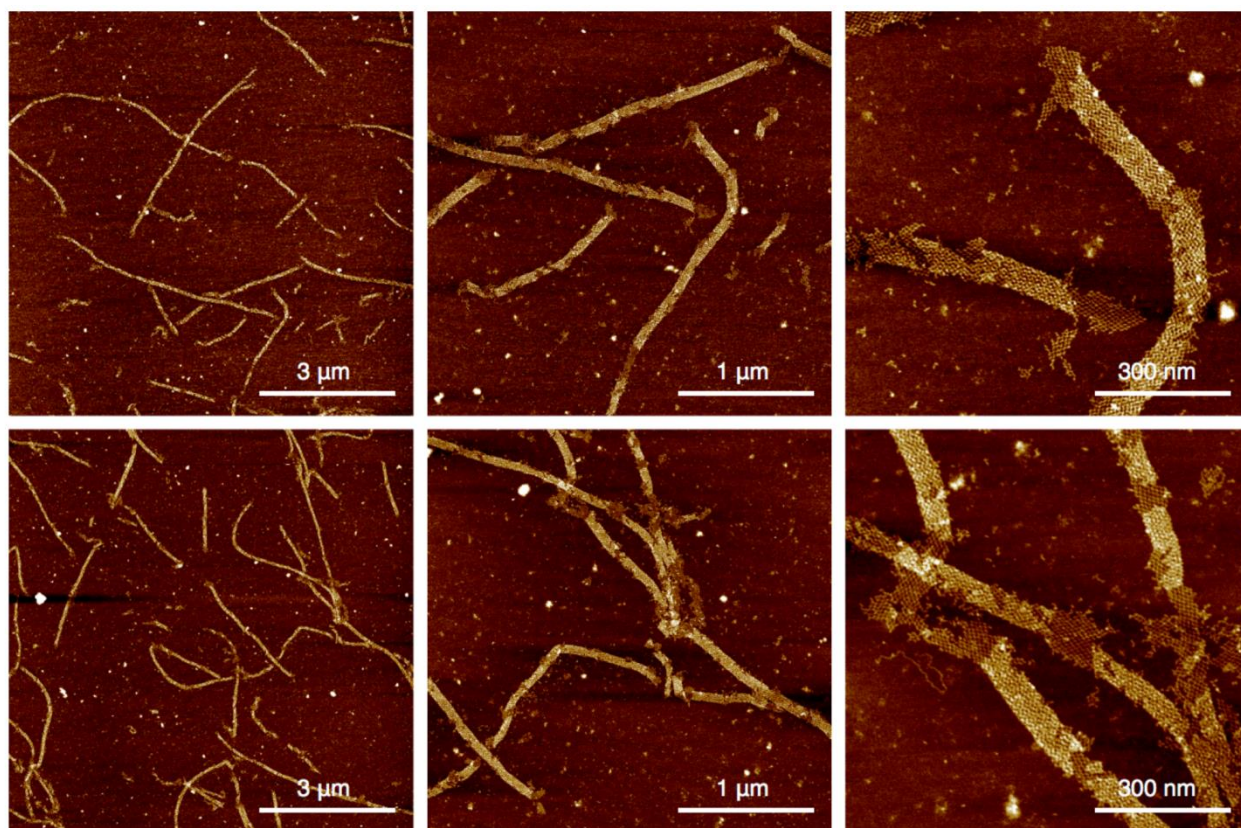
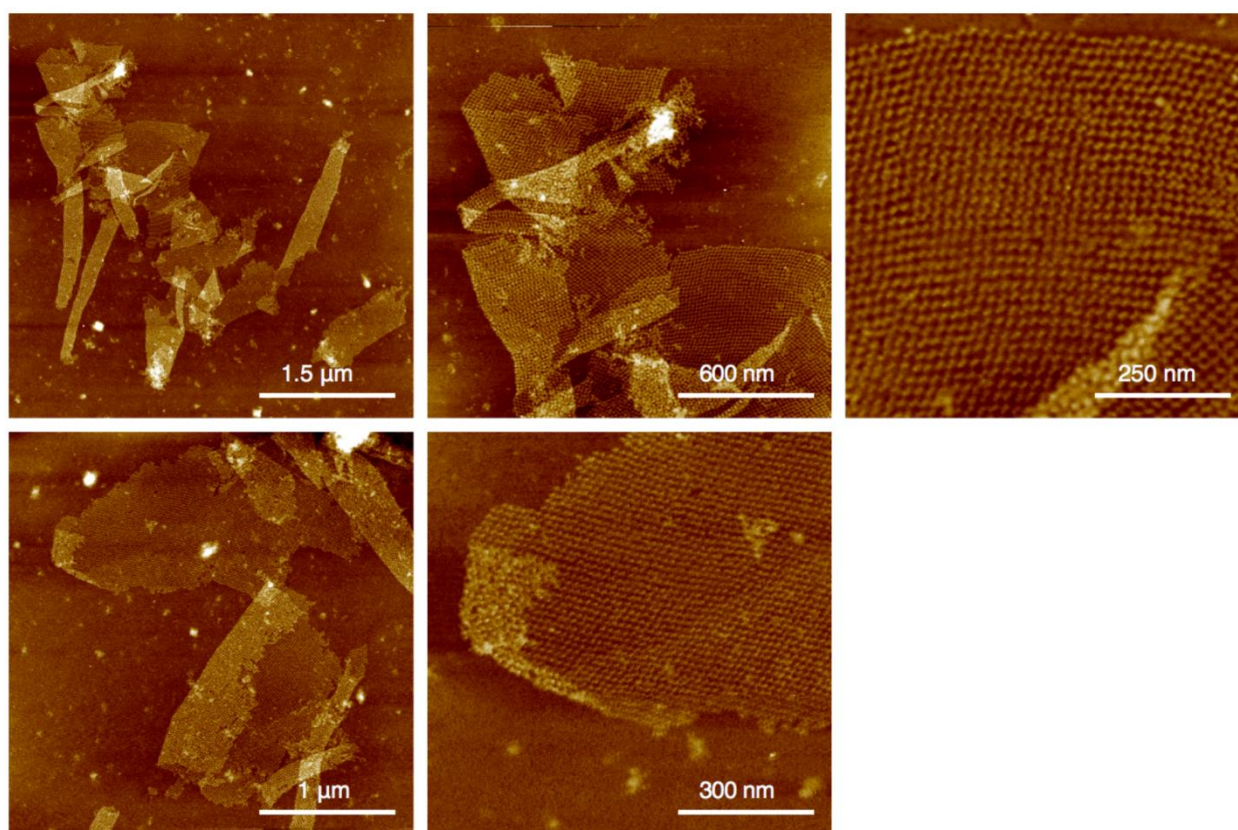


Figure. S21. AFM images of infinite cDAO-c84nt-E.

## SUPPORTING INFORMATION



**Figure. S22.** AFM images of infinite cDAO-c84nt-O.

## SUPPORTING INFORMATION

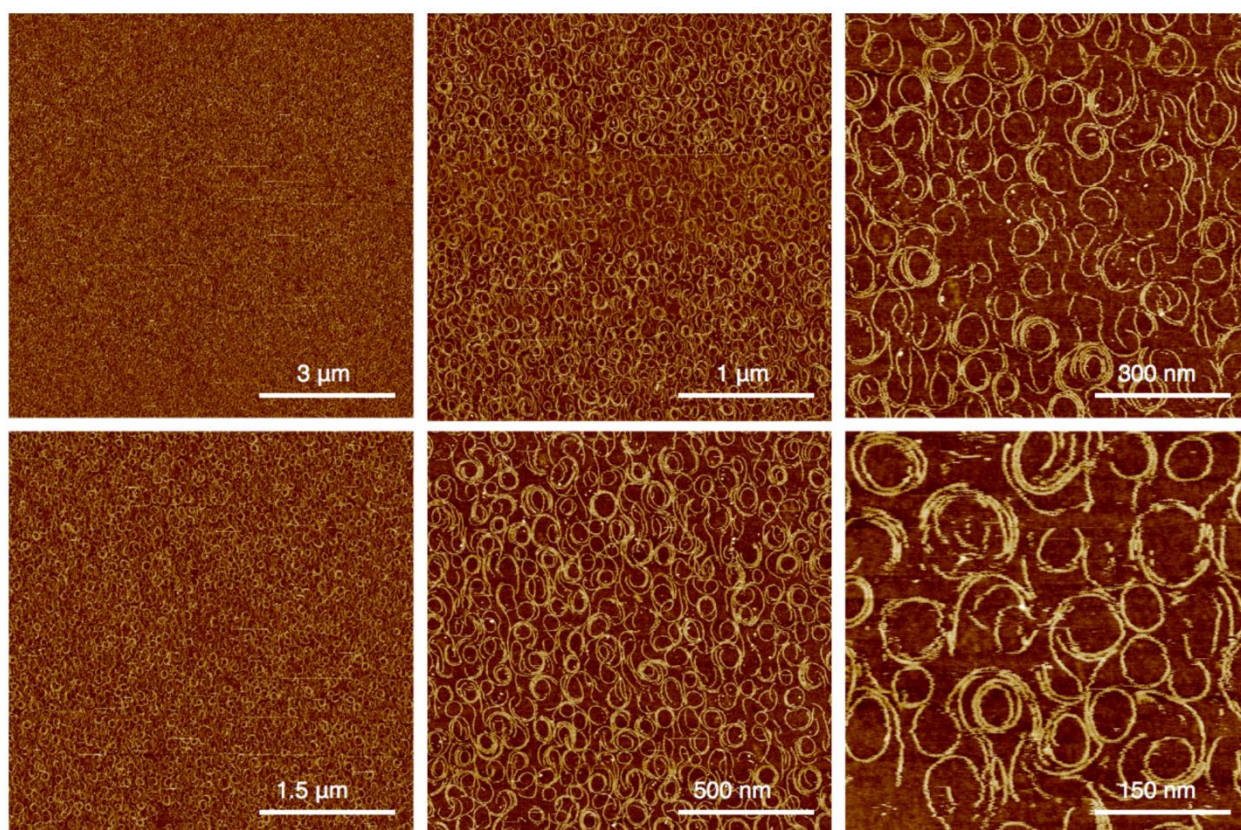


**Figure. S23.** AFM images of curved nanowires of acDAO-c64nt-E.



## SUPPORTING INFORMATION

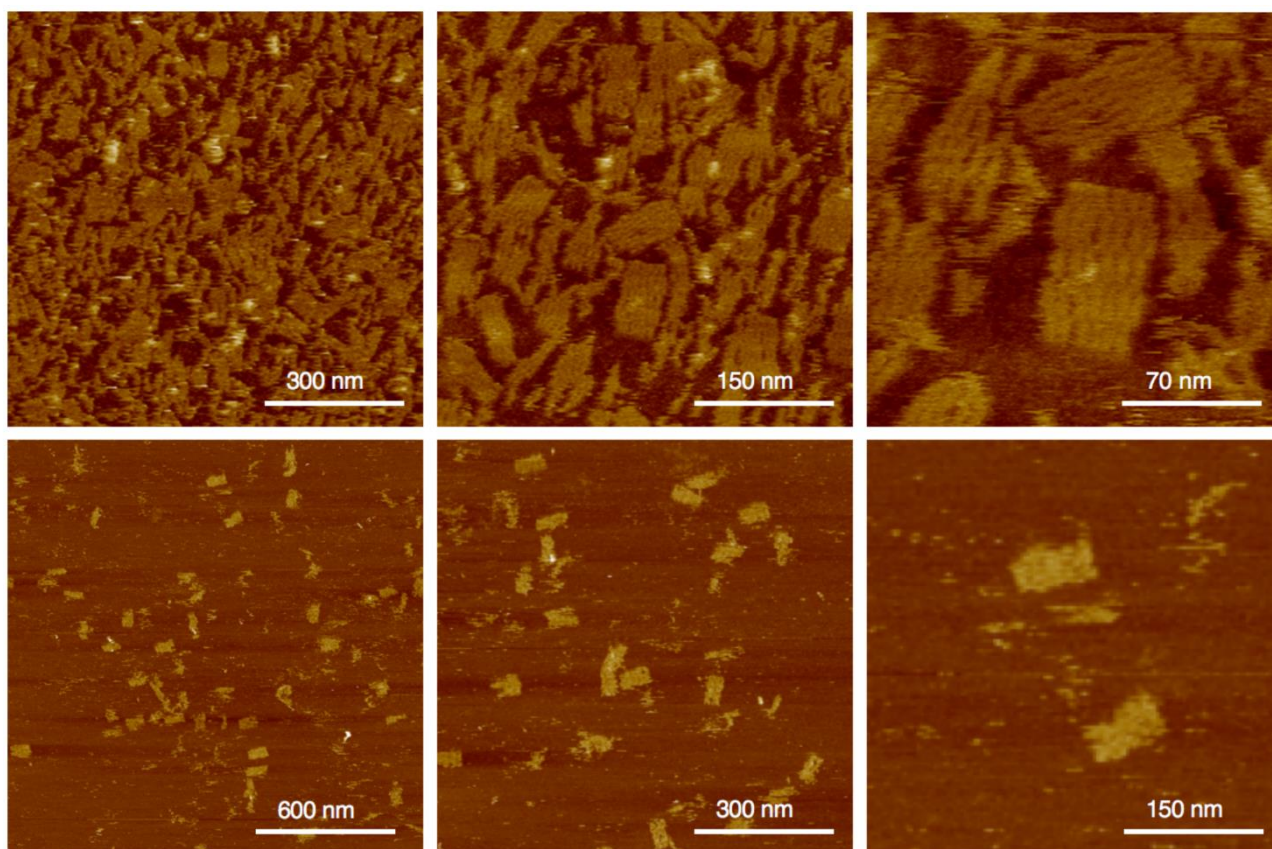


**Figure. S24.** AFM images of finite lattices of 5×6 patches of cDAO-c64nt-O. Upper three images are as-annealed products, both perfect finite rectangular lattices and partly-annealed lattices exist, and individual cDAO-c64nt tiles and inter-tile gaps can be clearly imaged. The yield of pure 5×6 cDAO-c64nt-O in the main text was estimated from the as-annealed samples supposing that all DNAs were deposited on the mica with the same probability. Lower three images are after purification, the background is clean and tiny assemblies are removed, however high-resolution details of cDAO-c64nt tiles and inter-tile gaps are much difficult to be captured.

## SUPPORTING INFORMATION

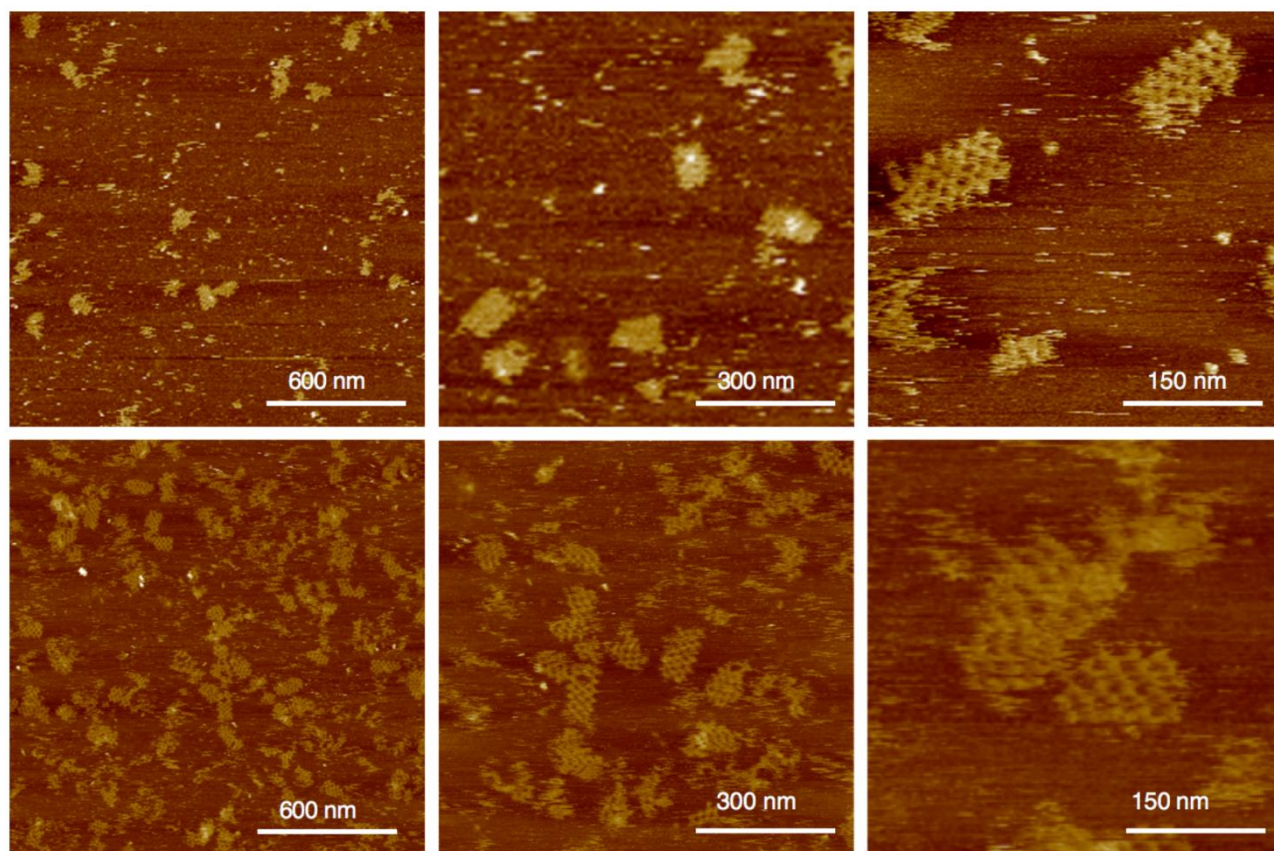


**Figure. S25.** AFM images of finite lattices of 5×6 patches of cDAO-c74&c84nt-O. Due to the design of cDAO-c74&c84nt-O, the inter-tile connections are spatially isolated double strands, thus the lattices are easy to be broken during the AFM imaging procedure.

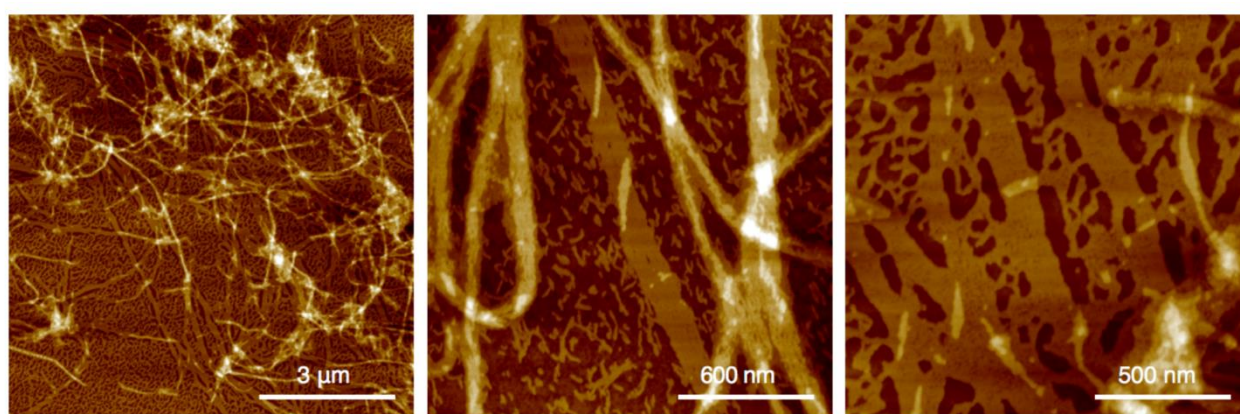


**Figure. S26.** AFM images of a control sample of infinite cDAO-64nt-O with a whole set of linear strands which are listed in Figure S10 with sequence details. Its assembly product is 2D amorphous aggregates along the double helical axes without details such as textures.

## References

- [1] E. Stahl, T. G. Martin, F. Praetorius, H. Dietz, *Angew. Chemie Int. Ed.* **2014**, *53*, 12735–12740.

SUPPORTING INFORMATION

---

- [2] C. Frontali, E. Dore, A. Ferrauto, E. Gratton, A. Bettini, M. R. Pozzan, E. Valdevit, *Biopolymers* **1979**, *18*, 1353–1373.
- [3] E. N. Trifonov, R. K.-Z. Tan, S. C. Harvey, *Structure & Expression: DNA Bending & Curvature*, Adenine Press, **1988**.
- [4] J. A. Schellman, S. C. Harvey, *Biophys. Chem.* **1995**, *55*, 95–114.
- [5] X. Li, W. Lehman, S. Fischer, *J. Struct. Biol.* **2010**, *170*, 313–318.
- [6] I. Usov, R. Mezzenga, *Macromolecules* **2015**, *48*, 1269–1280.
- [7] P. W. K. Rothmund, A. Ekani-Nkodo, N. Papadakis, A. Kumar, D. K. Fygenson, E. Winfree, *J. Am. Chem. Soc.* **2004**, *126*, 16344–16352.
- [8] D. Schiffels, T. Liedl, D. K. Fygenson, *ACS Nano* **2013**, *7*, 6700–6710.

**Author Contributions**

X.G. carried out all experiments, analyzed data and wrote the manuscript; X.M.W. complemented parts of the experiments; S.W. simulated the persistence length; S.J.X. conceived and designed the project, analyzed data and wrote the manuscript.